Charge-exchange processes in EBIT: implications for spectral analysis of few-electron Fe ions

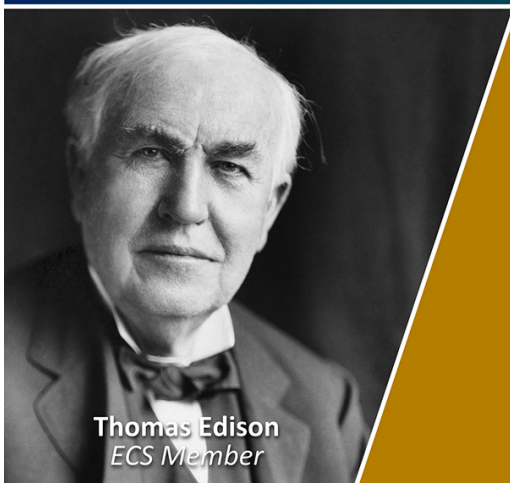View the article online for updates and enhancements.

THE 15TH INTERNATIONAL SYMPOSIUM ON ELECTRON BEAM ION SOURCES AND TRAPS
KIELCE, POLAND
27–30 AUGUST 2024

Charge-exchange processes in EBIT: implications for spectral analysis of few-electron Fe ions

Y. Yang [a,1,*] **Dipti** [a,b] **A.C. Gall** [c] **N. Brickhouse** [c] **H. Staiger** [a] **G. O'Neil** [d]
P. Szypryt [d] **A. Foster** [c] **D. Schultz** [e] **A. Naing** [b] **J.N. Tan** [b] **D. Swetz** [d] **M. Fogle** [f]
R. Smith [c] **Yu. Ralchenko** [b] and **E. Takacs** [a,b]

[a] *Clemson University,*
 118 Kinard Laboratory Clemson, SC, U.S.A.

[b] *National Institute of Standards and Technology,*
 Gaithersburg, MD 20899, U.S.A.

[c] *Center for Astrophysics | Harvard & Smithsonian,*
 Cambridge, MA 02138, U.S.A.

[d] *National Institute of Standards and Technology,*
 Boulder, CO 80305, U.S.A.

[e] *Northern Arizona University,*
 Flagstaff, AZ 86011, U.S.A.

[f] *Department of Physics, Auburn University,*
 Auburn, AL, 36849, U.S.A.

 E-mail: yang.yang@desy.de

ABSTRACT: Charge-exchange recombination with neutral atoms significantly influences the ionization balance in electron beam ion traps (EBIT) because its cross section is relatively large compared to cross sections of electron collision induced processes. Modeling the highly charged ion cloud requires the estimate of operating parameters, such as electron beam energy and density, the density of neutral atoms, and the relative velocities of collision partners. Uncertainty in the charge-exchange cross section can dominate the overall uncertainty in EBIT experiments, especially when it compounds with the uncertainties of experimental parameters that are difficult to determine. We present measured and simulated spectra of few-electron Fe ions, where we used a single charge-exchange factor to reduce the number of free parameters in the model. The deduction of the charge-exchange factor from the ratio of Li-like and He-like features allows for predicting the intensity of H-like lines in the spectra.

---

*Corresponding author.
[1] Present Address: Deutsches Elektronen Synchrotron DESY, Platanenallee 6, 15738 Zeuthen, Germany.

Contents

1 Introduction

Highly charged ions created in hot plasmas, both astrophysical and laboratory, produce a wealth of important diagnostic transitions. Spectra from these ions address questions ranging from star formation and turbulence in clusters of galaxies to temperature and chemical composition of confined laboratory plasmas [1–4]. Extracting valuable information from these spectra relies on using accurate atomic data in plasma modeling codes.

Electron beam ion traps (EBITs) are small-scale laboratory devices that create and trap highly charged ions for spectroscopic studies. The tuneable quasi-monoenergetic electron beam, which allows for charge state and excitation selectivity, makes this a powerful device well-suited for studies of electron impact excitation, ionization, radiative and dielectronic recombination, and identification of transitions from highly charged ions [5–7].

The combination of a highly controllable EBIT, with accurate modeling of emission of the non-Maxwellian plasma (e.g. [8, 9]), allows for the determination of important atomic data such as wavelengths, line intensities, and cross sections. These are used to benchmark, test, and improve plasma models of astrophysical and laboratory sources [10–12].

Modeling the EBIT plasma requires the understanding of underlying atomic processes that affect the spectral emission and the charge state distribution of the ion cloud. The charge state balance between ions is determined by a set of rate equations that connects the number density of ions via charge-changing interactions. These atomic processes decrease (recombination) or increase (ionization) the charge state of the ions through elementary collisional interactions with free electrons

of the electron beam, with other ions in the ion cloud, and neutral background atoms in the trap region. Conditions in the trap determine the relative importance of these processes. The general form of the rate equation connecting the different charge states takes the form of (see e.g. [13, 14]):

$$\frac{dN_i}{dt} = J_e \left(N_{i-1}\sigma_{i-1}^I - N_i\sigma_i^I + N_{i+1}\sigma_{i+1}^R - N_i\sigma_i^R \right) + n_0 \left(N_{i+1}\langle\sigma^{CX}v_r\rangle_{i+1} - N_i\langle\sigma^{CX}v_r\rangle_i \right) \quad (1.1)$$

In eq. (1.1) $J_e = n_e v$ denotes the electron current density, and N_{i+1}, N_i, and N_{i-1} are the ion number densities of neighboring charge states. σ^I represents the sum of cross sections corresponding to the collection of different ionization (I) processes including electron impact ionization (EII) and excitation followed by autoionization (EA). σ^R is the sum of cross sections for electron recombination (R) processes, like radiative recombination (RR) and dielectronic recombination (DR). In eq. (1.1) only single charge changing processes are assumed, although multiple ionization and recombination processes can also be included in a straightforward way.

In an EBIT charge exchange (CX) recombination occurs between ions and neutral atoms with number density n_0. Ion-ion recombination has a small cross section due to the strong repulsion between highly charged ions. charge exchange is a critical factor in the determination of the charge state balance.
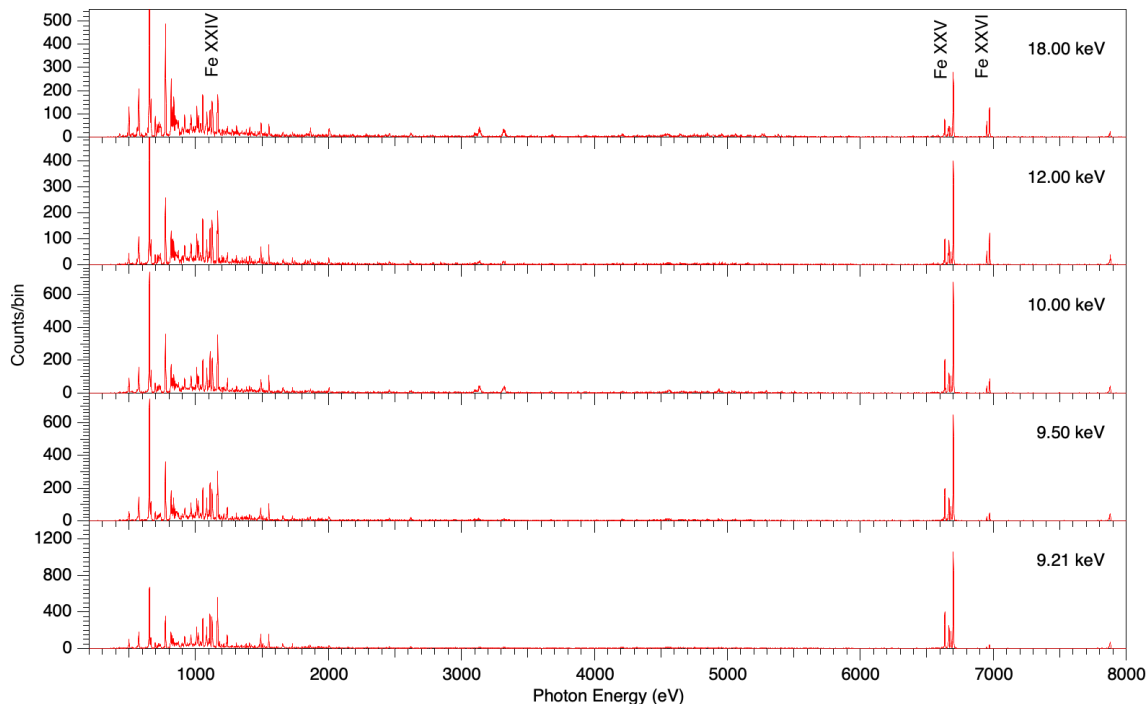
In the last two terms of eq. (1.1) the relative velocity of the ions and neutral atoms, v_r, is difficult to estimate, and the charge exchange cross section, σ^{CX}, has a large theoretical uncertainty. $\langle\sigma^{CX}v_r\rangle_i$ denotes the product of these two quantities averaged over the distribution of relative velocities. The large uncertainty associated with this factor poses a problem for the intensity analysis of emitted spectra [12, 15–18].

The temporal evolution of ion charge states in the EBIT has been a subject of several studies since the early days of EBIT research. Penetrante [14] performed ion extraction measurements and developed a model to calculate the time evolution of the ion charge states. Penetrante's code has been the basis of several early investigations and other groups later developed more up-to-date versions [13, 17, 19]. Estimating the values of EBIT operating parameters and the charge exchange rate remains the main challenge in these works.

In this paper, we will look into the problem of charge exchange with neutral atoms in the EBIT for the analysis of high energy-resolution, broadband, few-electron Fe x-ray spectra. We show that the combination of the charge exchange and electron beam related operating parameters can be reduced to a single factor that can be determined by comparing measured and calculated regions of spectra that include Li-like and He-like transitions. The factor can be applied to the detailed collisional-radiative analysis of H-like line intensities with good agreement between simulated and experimental spectra. Modeling of the EBIT plasma allows for the extraction of important atomic data, such as electron impact cross sections, from the measurements.

2   Experimental details

An extensive description of the vertically oriented versatile light source, NIST EBIT, can be found in [20]. The device is a cylindrically symmetric system used to produce and trap highly charged ions. It has three main components: the electron gun, drift-tube (trap), and collector assemblies. In the EBIT, a quasi mono-energetic electron beam is emitted from a curved, 3 mm diameter, barium-doped cathode in the electron-gun assembly. The electron beam is compressed to approximately 35 μm radius by a superconducting magnet capable of producing an up to 2.7 T field surrounding the trap.

Figure 1. TES spectra of Fe ions at five beam energies between 9.21 keV and 18.00 keV featuring Li-like transitions around 1.0 keV to 1.2 keV, He-like transitions around 6.6 keV to 6.7 keV, and H-like transitions near 7.0 keV x-ray energies.

The 10^{10} cm^{-3} to 10^{12} cm^{-3} density electron beam is accelerated toward the trap region that consists of three cylindrical drift tube electrodes capable of floating up to 30 kV voltage.

During highly charged Fe measurements, low-charge state ions are injected from a metal vapor vacuum arc (MeVVA) ion source [21] into the trapping region, where they are further ionized to highly charged states by electron impact ionization. The relative voltages placed on the three drift tube electrodes are used to trap the ions electrostatically in the axial direction. The lower drift tube is generally set to +500 V above the middle drift tube, and the upper drift tube is set to +250 V above the middle drift tube.

The potential difference between the cathode in the electron gun and the middle drift tube in the trap defines the nominal electron beam energy. The space charge offset [22, 23] lowers the nominal electron beam energy, and can be experimentally determined by comparing measured and theoretical spectra at beam energies where resonant processes take place. The details of such measurement for Fe spectra are included in [7], where the space charge corrected beam energy was determined to an uncertainty of 10 eV.

Experimental spectra presented in figure 1 were taken at five nominal electron beam energies between 9.21 keV to 18.00 keV in the 500 eV to 10 keV photon energy region with an x-ray energy resolution of about 5 eV throughout. The spectra were recorded with a 192-element x-ray microcalorimeter array based on transition-edge sensors (TES) [24]. Calibration was performed using K-alpha emission lines of Mg, Al, Fe, Co, and Ni produced by an external fluorescent source. Spectral lines near 1.1 keV mainly originate from Li-like ions. The well-known He-like and H-like transitions are seen at around 6.70 keV and 6.95 keV respectively.

3 Analysis of EBIT spectra

3.1 Line intensity ratios

In EBIT spectral analysis, line intensities are crucial for line identification, particularly in regions where spectral lines overlap or are close to each other (e.g., [5, 25]). The accurate determination of relative EBIT line intensities is also essential for measuring electron impact cross sections, where experimental intensity ratios, combined with theoretically calculated parameters, enable the evaluation of cross sections (e.g., [10–12]).

The intensity I of a measured spectral line can be expressed as

$$I = N_i PA \left(C_t C_d \right),$$ (3.1)

where I is proportional to the number of ions in the relevant charge state N_i, the population fraction P of these ions in the upper level of the atomic transition, and the transition probability A for decay to a lower level.

The unidirectional electron beam within the EBIT might produce anisotropic and polarized emission [26, 27], therefore, transition dependent factors can be collected into a correction factor (C_t), and detector related effects, such as spectrometer transmission, detector efficiency, and the solid angle can also be included in a separate correction factor (C_d).

N_i can be determined by the rate equation (eq. (1.1)), and the population fraction P can be calculated by collisional radiative codes specialized for the non-Maxwellian electron energy distribution of the EBIT, such as the NOMAD package [8] or the Flexible Atomic Code (FAC) [28]. They generally include excitation and cascade processes between energy levels of the ion or even those of neighboring charge states (e.g. via autoionization and recombination processes). The atomic data that goes into the transition, excitation, and recombination rates can come from reliable atomic structure codes, such as FAC itself [28] or the GRASP2K multi-configurational Dirac-Fock package [29].

Using eq. (3.1) the intensity ratios of two spectral lines (1 and 2) can be calculated as

$$\frac{I_1}{I_2} = \left(\frac{N_1 P_1 A_1}{N_2 P_2 A_2} \right) \left(\frac{C_{t1} C_{d1}}{C_{t2} C_{d2}} \right)$$ (3.2)

Simplifications can be applied for example when the upper levels of the transitions are the same ($P_1 = P_2$), or if the transitions originate from the same charge state and are close in energy ($C_{d1} = C_{d2}$), etc. In general, for well-calculable atomic transitions the main uncertainty in the calculated line intensity ratios comes from the limited knowledge of the physical quantities in the rate equation eq. (1.1).

3.2 Parameters of the rate equation

In eq. (1.1) the electron current density J_e, the density of neutral atoms n_0, the relative velocity between ions and neutral atoms v_r, and the charge exchange cross sections σ^{CX} are physical quantities that are difficult to estimate. Even with a well-designed neutral gas injection system that allows for the precise injection of atoms into the EBIT [30], the neutral density is difficult to determine and the theoretical calculations of the charge exchange cross sections of highly charged ions carry large uncertainties [15, 17]. Line intensity ratios of eq. (3.2) depend on these factors through eq. (1.1); therefore the comparison of measured and calculated values is limited by the estimation of these physical parameters.

The key concept in our analysis is that in evaluating line intensity ratios the unknown set of physical quantities can be reduced to a single factor that can be experimentally determined from the spectra. To show this, we begin by noting that, in equilibrium, the rate of change from charge state i to charge state $i + 1$ is equal to the rate of change from charge state $i + 1$ to i:

$$n_e v N_i \sigma_i^I = n_e v N_{i+1} \sigma_{i+1}^R + n_0 N_{i+1} \sigma_{i+1}^{CX} \bar{v}_r \tag{3.3}$$

In (3.3) $\bar{v}_r$ is the average neutral relative velocity inferred from (1.1). Rearranging equation (3.3) leads to

$$\frac{n_0 \bar{v}_r \sigma_{i+1}^{CX}}{n_e v} = \frac{N_i}{N_{i+1}} \sigma_i^I - \sigma_{i+1}^R \tag{3.4}$$

For transitions where the upper level is predominantly populated by electron impact excitation (as opposed to radiative cascades) the ratios of the number of ions in neighboring charge states can be expressed as

$$\frac{N_i}{N_{i+1}} = \frac{I_i^2 \sigma_{i+1}^{e1}}{I_{i+1}^1 \sigma_i^{e2}} \tag{3.5}$$

In eq. (3.5) σ_i^{ej} represent the excitation cross sections that populate the upper level of transition j in charge state i, and I_i^j is the intensity of the emitted spectral line.

Taking the example of Li-like and He-like transitions, combining eq. (3.4) and eq. (3.5), the line intensity ratios simplify to

$$\frac{I_{\mathrm{Li}}^2}{I_{\mathrm{He}}^1} = \left(\frac{n_0 \bar{v}_r \sigma_{\mathrm{He}}^{CX}}{n_e v} + \sigma_{\mathrm{He}}^R \right) \frac{1}{\sigma_{\mathrm{Li}}^I} \frac{\sigma_{\mathrm{Li}}^{e2}}{\sigma_{\mathrm{He}}^{e1}} \tag{3.6}$$

Depending on the particular purpose of the investigation eq. (3.6) can be used to theoretically predict line intensity ratios, determine cross sections from measurements, or estimate physical parameters of the EBIT. The term that generally carries that largest uncertainty in eq. (3.6) is $\frac{n_0 \bar{v}_r \sigma_i^{CX}}{n_e v}$. This is because of the large individual uncertainties associated with the hard-to-determine EBIT parameters, like the electron and neutral atom densities, the relative velocity of atoms and ions, and the charge exchange cross section itself.

Eq. (3.6) can also be used to express $\frac{n_0 \bar{v}_r \sigma_i^{CX}}{n_e v}$ and determine the value of the combination of these physical quantities more precisely than what the individual uncertainties would allow. The expression can be made more simple if we write the charge exchange cross section as a scaling constant σ^{CX} and a factor $Q^{CX}(q_i)$ that only depends on the q_i charge of the capturing ion.

$$\frac{n_0 \bar{v}_r \sigma^{CX}}{n_e v} Q^{CX}(q_i) \tag{3.7}$$

This expression is useful because the constant $\frac{n_0 \bar{v}_r \sigma^{CX}}{n_e v}$, determined from the ratio of one pair of lines, can be applied to other pairs regardless of their charge states, provided that $Q^{CX}(q_i)$ is known. From eq. (3.6) the uncertainty of this factor depends on the experimental uncertainty of the $\frac{I^1}{I^2}$ line intensity ratio, the uncertainties of the calculated electron impact cross sections, and the uncertainty associated with the $Q^{CX}(q_i)$ ion charge dependence of the charge exchange cross section. With the appropriate choice of transitions, the first two can be minimized, and the assessment of $Q^{CX}(q_i)$ can either be made theoretically or experimentally.

3.3 Charge exchange cross section

At NIST, collisional-radiative modeling of EUV and x-ray spectra for EBIT has been developed through numerous investigations over nearly two decades. The NOMAD non-Maxwellian code [8] is capable of time-dependent and equilibrium emission calculations by solving rate equations of the type of eq. (1.1) and including many thousand energy levels within the charge states.

For these studies, a simple $Q^{CX}(q_i) = q_i$ relationship is commonly used to reproduce both the spectral features and the charge state distribution of the EBIT ion cloud. The linear relationship, especially over a narrow range of charge states that the selectivity of EBIT devices provides, has also been realized in early charge exchange investigations [16, 31].

To further test the validity of this approach and assess the uncertainty associated with it, we have performed classical trajectory Monte Carlo (CTMC) simulations [32, 33] with the advanced nCTMC approach to determine the charge exchange cross sections between few-electron charge states of Fe and different neutral atoms and molecules. In the nCTMC model n electrons are bound by the sequential molecular orbital binding energies of the neutral collision partner [34–36]. Apart from single capture (SC), double capture (DC), triple capture (TC), and up to six-fold capture, all have been calculated and benchmarked by previous measurements. [35, 36].

With regard to multiple captures in a single collision, it was found that multiple electron captures are generally followed by Auger electron emission cascades, resulting in cross sections that are at least an order of magnitude smaller compared to those for single capture.

The calculations also provided absolute charge exchange cross section values for the few electron ions of Fe

$$\sigma_i^{CX} = \sigma^{CX} \times q_i \tag{3.8}$$

$$\sigma^{CX} = 0.71 \times 10^{-15} \, \text{cm}^2 \tag{3.9}$$

where q_i is the charge of the ion in units of the elementary charge. Since σ^{CX} is embedded in the $\frac{n_0 \bar{v}_r \sigma^{CX}}{n_e v}$ experimental factor, the main result of our charge exchange calculation in this section is the linearity of the cross section with the charge and the uncertainty that was used in our overall uncertainty estimates.

In general, charge exchange between neutral atoms and ions is an important process in determining plasma conditions and understanding the emission from both laboratory and astrophysical plasmas [33, 37, 38]. The need for charge exchange cross sections was realized in the 1970's [39, 40] when early measurements and empirical formulas were also published [41].

More recently, there has been an increased interest in charge exchange with the discovery of cometary and planetary x-rays due to the interaction of solar wind ions with neutral gases in these objects [37, 42, 43]. The interpretation of tokamak fusion spectra also highlighted the impact of charge exchange, as the intensity of He-like lines, which have potential diagnostic use, was found to strongly depend on the process [44].

Despite the need for cross sections by various fields, accurate values are generally not available for the charge states and species involved in plasma emission observations. Uncertainties of the charge exchange cross sections largely limit the understanding of the physics of these environments including laboratory measurements using EBITs. The use of the experimental charge exchange factor $\frac{n_0 \bar{v}_r \sigma^{CX}}{n_e v}$ in spectral analysis alleviates the need to know the absolute value of the charge exchange cross section when calculating relative line intensity ratios.

4 Uncertainty estimates

Extracted from eq. (3.6) the uncertainty of the $\frac{n_0 \bar{v}_r \sigma^{\mathrm{CX}}}{n_e v}$ charge exchange factor depends on the uncertainties of the calculated or tabulated electron impact cross sections and the experimental precision of the chosen line intensity ratio.

4.1 Radiative recombination

RR cross sections were derived from photoionization cross sections using the detailed balance principle and are the most straightforward to calculate with high accuracy compared to other electron-impact collision processes. The results of theoretical calculations for the photoionization of neutral atoms agree within 3% with measured values [45], and are anticipated to be better for highly-charged ions [46]. We have assumed 3% for the relative uncertainty of the RR cross sections in our Fe calculations.

4.2 Electron-impact excitation (EIE)

EIE cross sections were calculated using the FAC package based on the relativistic distorted-wave approach [9]. In evaluating the uncertainties due to the EIE for the determination of $\frac{n_0 \bar{v}_r \sigma^{\mathrm{CX}}}{n_e v}$ we note that in eq. (3.6) only ratios of excitation cross sections appear. As a result, large uncertainties that can hinder absolute EIE cross section determinations cancel out. For example, the oscillator strengths calculated with FAC for both H-like and He-like ions are higher than previously reported state-of-art theoretical calculations [47–50]. Scaling the absolute cross-sections with accurate oscillator strengths is a common practice and in our case, it was also used to estimate the uncertainty of the excitation cross section ratios. We have found that for the Li-like, He-like, and H-like ground state transitions in our study, including contributions related to the accuracy of the wave functions, the overall uncertainty is less than 4%.

4.3 Electron-impact ionization (EII)

EII cross sections were also calculated with the relativistic distorted-wave approach of the FAC package [9]. For Li-like Fe^{23+} ions, the ionization cross-section was measured at 4.66 keV electron impact energy [10], and agrees with our calculated value, showing a relative deviation of less than 3%. Our experiments were conducted at energies well above this, and since the relativistic distorted-wave method generally provides better agreement at higher energies, we assume that the uncertainty in the ionization cross-sections for Li-like ions is within 3%.

For He-like Fe^{24+} ions, the theoretical ionization cross-section values exhibit greater variation at the beam energies used in the current experiment, as these energies are relatively closer to the excitation thresholds of the considered transitions. Based on the variation in the theoretically calculated values [51–54], we estimate the uncertainty to be in the range of 10% to 20% depending on the method used.

4.4 Line intensity ratios

The uncertainties in the $\frac{I^1}{I^2}$ line intensity ratios are dominated by the photon count statistics collected under the peaks chosen for the evaluations. Corrections to the raw intensity values have been considered in the analysis including uncertainty estimates for these adjustments.

Corrected intensity ratios take into account contributions from anisotropic emission effects as well as cascades feeding of the upper levels of the transitions involved. Both emission and cascade effects were determined using detailed simulations performed with the collisional-radiative code NOMAD including magnetic sublevel atomic kinetics described in our previous publications [55, 56]. The maximum correction we found was less than 6% with an uncertainty of 10% of that value (0.6% of the intensity ratio).

Further corrections considered were the quantum efficiency of the detector and the x-ray transmission through the windows of the spectrometer [24]. We have used vendor provided measurements and uncertainties for the material thicknesses involved and the NIST maintained mass attenuation coefficient tables for the calculations [57]. The overall uncertainty of the line intensity ratios due to these corrections is on the order of 0.1%.

5 He-like and H-like Fe

5.1 Charge exchange factor

For the determination of the $\frac{n_0 \bar{v}_r \sigma^{CX}}{n_e v}$ experimental factor and its uncertainty for the analysis of the few-electron Fe spectra in figure 1 we have selected two strong Li-like $1s^2 2s$-$1s^2 3p$ transitions of table 1 in the 1.1 keV–1.2 keV x-ray region and the well known He-like $1s^2$ $^1S_0$-$1s2p$ $^1P_1$ w line.

Spectral lines of table 1 have been identified in the spectra of figure 1 and fitted with Gaussian functions to determine their intensities with the corrections explained in section 4.4 including the associated uncertainties.

Simulated spectra were generated by the non-Maxwellian collisional-radiative modeling code NOMAD [8] at various experimental parameter $\frac{n_0 \bar{v}_r \sigma^{CX}}{n_e v}$ values, using the electron impact cross sections described in the preceding section. Experimental and calculated line intensities were normalized to the intensity of the w line. The value of the $\frac{n_0 \bar{v}_r \sigma^{CX}}{n_e v}$ parameter was deduced from the matching intensities of the experimental and calculated Li-like transitions.
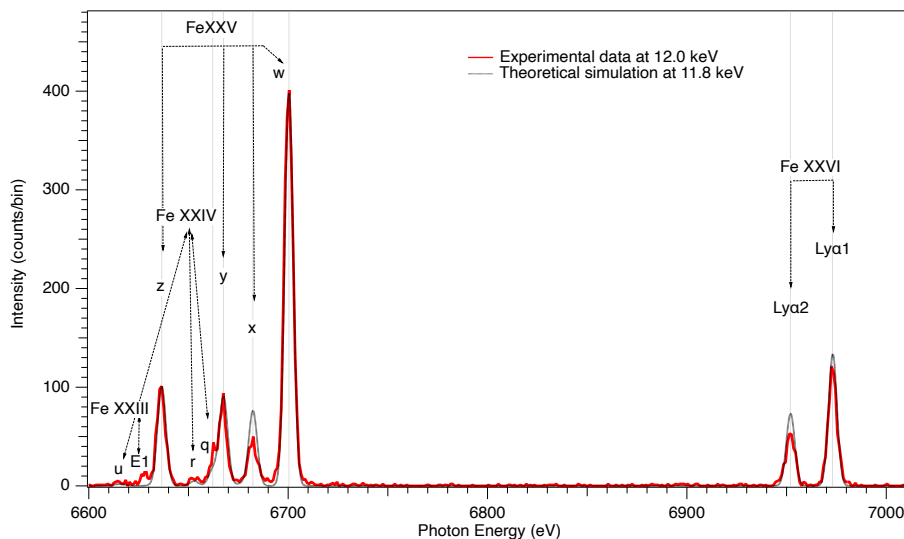
Since the charge exchange electron capture can depend on the orbital quantum number (l), three different models were compared to study the effect of l-distributions. (i) The CX electrons were captured directly into the ground state of the recombined ion. (ii) The electrons were captured into the $n = 11$ shell and were distributed according to the statistical weights ($2l+1$) of the l levels. (iii) The (n, l) populations were set according to the cross sections calculated using the CTMC method. All three models resulted in the same $\frac{n_0 \bar{v}_r \sigma^{CX}}{n_e v}$ parameter within the experimental statistical uncertainties of the measured line intensity ratios.

Table 1. Selected transitions of Li-like and He-like Fe [58].

Energy(eV)	Transition	Ref.
1162.70	Li-like: $1s^2 2s\ ^2S_{\frac{1}{2}} - 1s^2 3p\ ^2P_{\frac{1}{2}}$	[59–61]
1167.60	Li-like: $1s^2 2s\ ^2S_{\frac{1}{2}} - 1s^2 3p\ ^2P_{\frac{3}{2}}$	[59–61]
6700.44	He-like: $1s^2\ ^1S_0 - 1s2p\ ^1P_1$	[62]

5.2 Modeling of experimental spectra

With the charge exchange factor determined from the Li-like to He-like spectra, NOMAD simulations of the He-like and H-like spectral regions of the x-ray emission can be performed. Figure 2 compares the calculated and experimental spectra between 6600 eV and 7000 eV x-ray photon energies at 12.00 keV electron beam energy. The closely matching relative theoretical and measured spectra depicted in figure 2 indicate that the charge state balance calculation based on the $\frac{n_0 \bar{v}_r \sigma^{CX}}{n_e v}$ factor is a viable approach in EBIT spectral analysis.

Figure 2. Comparison of theoretical and experimental line intensities for He-like and H-like Fe lines at a beam energy of 12.00 keV. The small mismatch between the measured and calculated H-like Lyα intensities are due to the theoretical EII cross section of He-like Fe.

The relative theoretical intensity (2.98) and the measured intensity (3.23 ± 0.16) of the He-like w line with respect to the H-like Lyα1 line show a slight disagreement. This discrepancy most likely stems from inaccurate theoretical He-like EII cross-section values used in the model. We believe that the uncertainties in the experimental line intensity ratios and the experimental factor highlight the possibility for an improved determination of the ionization cross section of He-like Fe ions.

In the analysis of the Lyα2 line intensity, a contribution from the magnetic dipole transition (M1) $2s_{1/2} - 1s_{1/2}$ transition also needs to be taken into account. The energy separation between the two transitions in iron is only 0.03 eV [63], which cannot be resolved in our spectrum.

6 Conclusions

Plasma modeling plays a critical role in interpreting and extracting atomic data from measured spectra. A fundamental aspect of modeling hot plasmas is understanding the charge state balance. However, this remains challenging due to the difficulty in determining key experimental parameters, such as the density of neutral atoms and the relative velocities of the collision partners. In this work, we simplified the analysis of EBIT spectra by introducing a single unknown parameter into our model, which allowed us to determine the charge-exchange factor for a few-electron Fe EBIT plasma across a range of electron beam energies.

To test our approach we analyzed x-ray spectra of highly charged Fe ions recorded by a 192 transition-edge sensor (TES) x-ray microcalorimeter array on the NIST EBIT. By integrating the charge-exchange factor into a detailed collisional-radiative model, we achieved good agreement between the simulated and experimental spectra of few-electron Fe. Through a comparison of measured and calculated line intensity ratios, we quantified the uncertainties involved in calculating the charge-exchange factor. This not only validates the model, but also enables the precise experimental determination of the electron-impact ionization (EII) cross section for He-like Fe, owing to the control of uncertainties throughout the analysis. These results are being published in a separate work [64].

Acknowledgments

References

[1] P. Beiersdorfer, *Highly charged ions in magnetic fusion plasmas: research opportunities and diagnostic necessities*, *J. Phys. B* **48** (2015) 144017.

[2] A.J. Fairchild et al., *High-resolution laboratory measurements of M-shell Fe EUV line emission using EBIT-I*, *Eur. Phys. J. D* **78** (2024) 99 [`arXiv:2408.14454`].

[3] J. Clementson and P. Beiersdorfer, *Investigation of Dielectronic Recombination Satellite Emission to Fe XVIII for Temperature Measurements of Stellar Atmospheres*, *Astrophys. J.* **763** (2013) 54.

[4] Hɪᴛᴏᴍɪ collaboration, *Atomic data and spectral modeling constraints from high-resolution X-ray observations of the Perseus cluster with Hitomi*, *Publ. Astron. Soc. Jap.* **70** (2018) 12 [`arXiv:1712.05407`].

[5] C. Suzuki et al., *Identifications of extreme ultraviolet spectra of Br-like to Ni-like neodymium ions using an electron beam ion trap*, *J. Phys. B* **54** (2021) 015001.

[6] Y. Yang et al., *Observations and identifications of extreme ultraviolet spectra of Ca-like to Na-like neodymium ions using an electron beam ion trap*, *J. Phys. B* **56** (2023) 175003.

[7] Y. Yang et al., *Determination of Electron Beam Energy in Measuring the Electron-Impact Ionization Cross Section of He-like Fe^{24+}*, *Atoms* **11** (2023) 44.

[8] Y.V. Ralchenko and Y. Maron, *Accelerated Recombination due to Resonant Deexcitation of Metastable States*, *J. Quant. Spectrosc. Radiat. Trans.* **71** (2001) 609 [`physics/0105092`].

[9] M.F. Gu, *The flexible atomic code*, *Can. J. Phys.* **86** (2008) 675.

[10] K. Wong et al., *Electron-impact ionization of lithiumlike ions: Ti^{19+}, V^{20+}, Cr^{21+}, Mn^{22+}, and Fe^{23+}*, *Phys. Rev. A* **48** (1993) 2850.

[11] R.E. Marrs, S.R. Elliott and D.A. Knapp, *Production and trapping of hydrogenlike and bare uranium ions in an electron beam ion trap*, *Phys. Rev. Lett.* **72** (1994) 4082.

[12] R.E. Marrs, S.R. Elliott and J.H. Scofield, *Measurement of electron-impact ionization cross sections for hydrogenlike high-Z ions*, *Phys. Rev. As* **56** (1997) 1338.

[13] F. Currell and G. Fussmann, *Physics of Electron Beam Ion Traps and Sources*, *IEEE Trans. Plasma Sci.* **33** (2005) 1763.

[14] B.M. Penetrante et al., *Evolution of ion-charge-state distributions in an electron-beam ion trap*, *Phys. Rev. As* **43** (1991) 4861.

[15] N. Selberg, C. Biedermann and H. Cederquist, *Semiempirical scaling laws for electron capture at low energies*, *Phys. Rev. As* **54** (1996) 4127.

[16] R. Phaneuf, *Electron capture by slow Fe^{q+} ions from hydrogen atoms and molecules*, *Phys. Rev. A* **28** (1983) 1310.

[17] Y.F. Liu, K. Yao, R. Hutton and Y. Zou, *Numerical simulations using an improved calculational scheme for ion charge state distribution and ion temperature evolution in an EBIT*, *J. Phys. B* **38** (2005) 3207.

[18] Y. Ralchenko et al., *EUV spectra of highly-charged ions W^{54+}-W^{63+} relevant to ITER diagnostics*, *J. Phys. B* **41** (2008) 021003.

[19] X. Lu, H. Watanabe and F.J. Currell, *Numerical simulation of the charge balance in an EBIT*, *Nucl. Instrum. Meth. B* **205** (2003) 234.

[20] J.D. Gillaspy, *First results from the EBIT at NIST*, *Phys. Scripta T* **71** (1997) 99.

[21] G.E. Holland et al., *Low jitter metal vapor vacuum arc ion source for electron beam ion trap injections*, *Rev. Sci. Instrum.* **76** (2005) 073304.

[22] M.A. Levine et al., *The Electron Beam Ion Trap: A New Instrument for Atomic Physics Measurements*, *Phys. Scripta T* **22** (1988) 157.

[23] J.V. Porto, I. Kink and J.D. Gillaspy, *Direct imaging of highly charged ions in an electron beam ion trap*, *Rev. Sci. Instrum.* **71** (2000) 3050.

[24] P. Szypryt et al., *A transition-edge sensor-based x-ray spectrometer for the study of highly charged ions at the National Institute of Standards and Technology electron beam ion trap*, *Rev. Sci. Instrum.* **90** (2019) 123107 [`arXiv:2005.05483`].

[25] R. Silwal et al., *Identification and Plasma Diagnostics Study of Extreme Ultraviolet Transitions in Highly Charged Yttrium*, *Atoms* **5** (2017) 30.

[26] M.F. Gu, D.W. Savin and P. Beiersdorfer, *Effects of electron spiralling on the anisotropy and polarization of photon emission from an electron beam ion trap*, *J. Phys. B* **32** (1999) 5371.

[27] P. Beiersdorfer et al., *Measurement and interpretation of the polarization of the x-ray line emission of heliumlike Fe XXV excited by an electron beam*, *Phys. Rev. As* **53** (1996) 3974.

[28] M.F. Gu, *The flexible atomic code*, *AIP Conf. Proc.* **730** (2004) 127.

[29] P. Jönsson et al., *New version: GRASP2K relativistic atomic structure package*, *Comput. Phys. Commun.* **184** (2013) 2197.

[30] K. Fahy et al., *Extreme-ultraviolet spectroscopy of highly charged xenon ions created using an electron-beam ion trap*, *Phys. Rev. As* **75** (2007) 032520.

[31] R.K. Janev and H. Winter, *State-selective electron capture in atom-highly charged ion collisions*, *Phys. Rept.* **117** (1985) 265.

[32] R.E. Olson and A. Salop, *Charge-transfer and impact-ionization cross sections for fully and partially stripped positive ions colliding with atomic hydrogen*, *Phys. Rev. A* **16** (1977) 531.

[33] S. Otranto, R.E. Olson and P. Beiersdorfer, *Cometary x-rays: line emission cross sections for multiply charged solar wind ion charge exchange*, *J. Phys. B* **40** (2007) 1755.

[34] J. Machacek et al., *Solar-wind ion-driven x-ray emission from cometary and planetary atmospheres: Measurements and theoretical predictions of charge-exchange cross-sections and emission spectra for $O^{6+}+H_2O$, CO, CO_2, CH_4, N_2, NO, N_2O, and Ar*, *Astrophys. J.* **809** (2015) 75.

[35] J. Simcic et al., *Measurement and calculation of absolute single- and multiple-charge-exchange cross sections for Fe^{q+} ions impacting CO and CO_2*, *Phys. Rev. A* **81** (2010) 062715.

[36] J. Simcic et al., *Measurement and calculation of absolute single and multiple charge exchange cross sections for Fe^{q+} ions impacting H_2O*, *Astrophys. J.* **722** (2010) 435.

[37] P. Beiersdorfer et al., *Laboratory Simulation of Charge Exchange-Produced X-ray Emission from Comets*, *Science* **300** (2003) 1558.

[38] C. Lisse et al., *Discovery of X-ray and Extreme Ultraviolet Emission from Comet C/Hyakutake 1996 B2*, *Science* **274** (1996) 205.

[39] G. Steigman, *Charge transfer reactions in multiply charged ion-atom collisions*, *Astrophys. J.* **199** (1975) 642.

[40] W.H. Louisell, W.B. McKnight and M.O. Scully, *Analysis of a soft-x-ray laser with charge-exchange excitation*, *Phys. Rev. As* **11** (1975) 989.

[41] A. Müller and E. Salzborn, *Scaling of cross sections for multiple electron transfer to highly charged ions colliding with atoms and molecules*, *Phys. Lett. A* **62** (1977) 391.

[42] P. Beiersdorfer et al., *X-Ray Velocimetry of Solar Wind Ion Impact on Comets*, *Astrophys. J. Lett.* **549** (2001) L147.

[43] A. Bhardwaj et al., *X-rays from solar system objects*, *Planet. Space Sci.* **55** (2007) 1135 [arXiv:1012.1088].

[44] O. Marchuk et al., *Recombination mechanisms in He-like argon spectra measured in low-density plasmas*, *J. Phys. B* **40** (2007) 4403.

[45] E.B. Saloman, J.H. Hubbell and J.H. Scofield, *X-ray attenuation cross sections for energies 100 eV to 100 keV and elements Z = 1 to Z = 92*, *Atom. Data Nucl. Data Tabl.* **38** (1988) 1.

[46] S. Chantrenne, P. Beiersdorfer, R. Cauble and M.B. Schneider, *Measurement of electron impact excitation cross sections for heliumlike titanium*, *Phys. Rev. Lett.* **69** (1992) 265.

[47] G. Drake, *Unified relativistic theory for frequencies and transition rates in heliumlike ions*, *Phys. Rev. A* **19** (1979) 1387.

[48] W.R. Johnson and U.I. Safronova, *Revised transition probabilities for Fe XXV: Relativistic CI calculations*, *Atom. Data Nucl. Data Tabl.* **93** (2007) 139.

[49] V.G. Pal'chikov, *Relativistic Transition Probabilities and Oscillator Strengths in Hydrogen-like Atoms*, *Phys. Scripta* **57** (1998) 581.

[50] R.V. Popov and A.V. Maiorova, *Relativistic calculations of one-photon transition probabilities in hydrogen-like ions*, *Opt. Spectrosc.* **122** (2017) 366.

[51] D. Fang et al., *Electron-ion collisional ionization cross sections for the H and He isoelectronic sequences*, *Atom. Data Nucl. Data Tabl.* **61** (1995) 91.

[52] S.M. Younger, *Electron impact ionization rate coefficients and cross sections for highly ionized iron*, *J. Quant. Spectrosc. Radiat. Transf.* **27** (1982) 541.

[53] H.L. Zhang and D.H. Sampson, *Rapid relativistic distorted-wave approach for calculating cross sections for ionization of highly charged ions*, *Phys. Rev. A* **42** (1990) 5378.

[54] D.V. Fursa, C.J. Bostock, I. Bray and C.J. Fontes, *Calculations of electron-impact ionisation of Fe^{25+} and Fe^{24+}*, *J. Phys. B* **49** (2016) 184001.

[55] A.C. Gall et al., *Measurements of linear polarization of satellite transitions from Li- and Be-like Ar ions*, *J. Phys. B* **53** (2020) 145004.

[56] Dipti et al., *Linear polarization of anisotropically excited x-ray lines from the n = 2 complex in He-like Ar^{16+}*, *J. Phys. B* **53** (2020) 115701.

[57] J.H. Hubbell and S. Seltzer, *X-Ray Mass Attenuation Coefficients*, NIST Standard Reference Database 126 (2004) [`DOI:10.18434/T4D01F`].

[58] A. Kramida, Y. Ralchenko, J. Reader and NIST ASD Team, NIST Atomic Spectra Database (ver. 5.5.1) (2019).

[59] J. Reader, J. Sugar, N. Acquista and R. Bahr, *Laser-produced and tokamak spectra of lithiumlike iron, Fe^{23+}*, *J. Opt. Soc. Am. B* **11** (1994) 1930.

[60] L. Armstrong Jr., W.R. Fielder and D.L. Lin, *Relativistic effects on transition probabilities in the Li and Be isoelectronic sequences*, *Phys. Rev. A* **14** (1976) 1114.

[61] Y.-K. Kim and J.P. Desclaux, *Relativistic f values for the resonance transitions of Li- and Be-like ions*, *Phys. Rev. Lett.* **36** (1976) 139.

[62] K. Kubiček et al., *Transition energy measurements in hydrogenlike and heliumlike ions strongly supporting bound-state QED calculations*, *Phys. Rev. A* **90** (2014) 032508.

[63] K. Wong, P. Beiersdorfer, K. Reed and A. Osterheld, *Measurement of the relative intensity of the Ly-(alpha) lines in Fe^{25+}*, Tech. Rep., Lawrence Livermore National Lab. (LLNL), Livermore, CA, U.S.A. (2002).

[64] Y. Yang et al., *Measurement of the Electron Impact Ionization Cross Section of Helium-like Iron*, submitted to *Astrophys. J.*.